Discrete Vector Solitons in Kerr Nonlinear Waveguide Arrays

Joachim Meier,[1] Jared Hudock,[1] Demetrios Christodoulides,[1] George Stegeman,[1] Y. Silberberg,[2] R. Morandotti,[3] and J. S. Aitchison[4]

[1]*CREOL/School of Optics, University of Central Florida, Orlando, Florida, 32816, USA*
[2]*Department of Physics of Complex Systems, The Weizmann Institute of Science, 76100 Rehovot, Israel*
[3]*Institut National de la Recherché Scientifique, Université du Québec, Varennes, Québec, Canada J3X 1S2*
[4]*Department of Electrical and Computer Engineering, University of Toronto, Toronto, Ontario, Canada M5S 3G4*

(Received 24 March 2003; published 3 October 2003)

We report the first experimental observation of discrete vector solitons in AlGaAs nonlinear waveguide arrays. These self-trapped states are possible through the coexistence of two orthogonally polarized fields and are stable in spite of the presence of four-wave mixing effects. We demonstrate that at sufficiently high power levels the two polarizations lock into a highly localized vector discrete soliton that would have been otherwise impossible in the absence of either one of these two components.

DOI: 10.1103/PhysRevLett.91.143907 PACS numbers: 42.82.Et, 42.65.Sf, 42.65.Tg

One-dimensional nonlinear lattices are known to exhibit a host of unique properties that have no analog whatsoever in homogeneous systems. One of the most intriguing outcomes of nonlinearity in such a periodic environment is perhaps the existence of self-localized entities — better known as *discrete solitons* (DSs) [1–4]. In nonlinear optics, DSs find their most straightforward manifestation in coupled nonlinear waveguide arrays as first predicted in Ref. [2]. In the linear regime, light in these periodic waveguide lattices propagates from site to site due to evanescent field coupling among adjacent waveguides [5]. It is interesting to note that this discrete diffraction (or tunneling) mechanism has much in common with electron transport processes in semiconductor crystals when described within the so-called tight-binding approximation [6]. Therefore, as a direct result of the array discreteness, linear optical wave propagation is associated with allowed and forbidden bands within the Brillouin zone [7]. At higher power levels, however, the nonlinear array is perturbed and this local defect allows a DS to form. Such DSs have been experimentally observed in arrays with Kerr [8], quadratic [9], and photorefractive nonlinearities [10] in both one and two transverse dimensions. Thus far several classes of DSs, some entirely unique to discrete systems, have been predicted. These include both bright and dark in-phase and staggered DSs in self-focusing and defocusing arrays [2,11] and higher-order Floquet-Bloch solitons [12].

Vector discrete solitons make up another important family of such self-localized states [7,13]. A vector soliton exists through the mutual trapping of two or more nonlinearly interacting wave packets, and thus this composite structure is possible only provided that all its components are simultaneously present [14–17]. Composite DSs have also been predicted in optical waveguide arrays with either Kerr or quadratic nonlinearity [13,18]. In quadratically nonlinear waveguide arrays, stable domain walls and quasirectangular solitons have been suggested, whereas in Kerr arrays with Manakov-like interactions, bright-bright and dark-antidark vector soliton pairs were theoretically identified in both 1D and 2D systems [7,19]. Discrete vector interactions in two-dimensional array networks have also shown considerable promise toward implementing all-optical switching, routing, and logic functions [20]. However, until now, no experimental observations of vector discrete solitons have ever been reported in *any physical system.*

In this Letter, we report the first experimental observation of vector discrete solitons consisting of two coherently coupled orthogonal polarizations in Kerr nonlinear waveguide arrays. We find that these vector solitons can propagate in a stable fashion, in spite of four-wave mixing effects, provided that the two appropriate polarization components (TE/TM) are in-phase at the input of the array. Our experiment demonstrates self-localization when both polarization components are present whereas in the absence of either the TE or TM polarization discrete diffraction occurs. The stability of these vector discrete solitons under the action of four-wave mixing power exchange was also investigated by varying the relative input phase between the two polarizations. Our analysis is in good agreement with the experimental results.

Our experiments were carried out in a 13.9 mm long AlGaAs waveguide array similar to that previously used to observe scalar solitons [8]. The wavelength used to excite this Kerr nonlinear array is $\lambda_0 = 1.55$ μm, i.e., below half the semiconductor's band gap so as to minimize nonlinear absorption effects. The Kerr coefficient is taken to be $\hat{n}_2 = 1.5 \times 10^{-13}$ cm^2/W, and at this wavelength, the effective cross-sectional area of each waveguide is $A_{\text{eff}} = 4.7$ μm^2. The coupling constant among adjacent waveguide sites is $\kappa = 0.336$ mm^{-1}, and the linear birefringence in every channel is estimated to be $n_x - n_y = 1.8 \times 10^{-4}$. In our system, the slow axis (n_x) is associated with the TE polarization.

From coupled mode theory, the wave dynamics of the two orthogonally polarized fields can be described by the following pair of discrete evolution equations:

$$
\begin{aligned}
i\frac{da_n}{d\zeta} + a_n + \gamma(a_{n+1} + a_{n-1}) + \\
[|a_n|^2 + A|b_n|^2]a_n + Bb_n^2 a_n^* = 0, \\
i\frac{db_n}{d\zeta} - b_n + \gamma(b_{n+1} + b_{n-1}) + \\
[|b_n|^2 + A|a_n|^2]b_n + Ba_n^2 b_n^* = 0.
\end{aligned} \tag{1}
$$

In the above equations, a_n and b_n are the normalized slowly varying field envelopes of the TE and TM polarized waves and are related to the actual fields via $(a_n, b_n) = [n_2/(n_x - n_y)]^{1/2}(E_{nx}, E_{ny})$. The Kerr coefficient used in Eqs. (1) is given by $n_2 = \hat{n}_2 n/2\eta_0$, where η_0 is the vacuum intrinsic impedance and for this material the refractive index is about $n = 3.3$. The coupling coefficient γ is normalized with respect to the birefringence, $\gamma = 2\kappa/[k_0(n_x - n_y)]$, and in modeling this system, we have assumed that it is the same for both polarizations. Equation (1) implicitly describes self-phase, cross-phase modulation, and four-wave mixing processes. The values of the A, B coefficients, respectively, associated with cross-phase modulation and four-wave mixing effects (as obtained from the AlGaAs $\chi^{(3)}$tensor), are approximately equal to $A \approx 1$ and $B \approx 1/2$. The normalized distance ζ is related to the actual z coordinate via $\zeta = k_0 z(n_x - n_y)/2$, and the birefringence of the array is reflected in the second terms of Eqs. (1).

To gain insight into the dynamics of vector discrete solitons, it is useful to first theoretically analyze the array system using Eqs. (1). To identify the vector DSs of this system, we assume that the soliton solutions have the form $(a_n, b_n) = (X_n, Y_n)\exp(iq\zeta)$. The nonlinear difference equations that result after the substitution of these forms into Eqs. (1) are then solved using Newtonian relaxation techniques. Here, we concentrate on the most primitive vector DS classes that are directly relevant to our experimental observations. After obtaining the vector DS solutions of Eqs. (1), the corresponding family is mapped on a $P - \Delta$ diagram, where $P = (n_x - n_y) \times (A_{\text{eff}}/\hat{n}_2)\sum(|a_n|^2 + |b_n|^2)$ is the total power in the waveguide array as conveyed by both polarizations and $\Delta = (k_0 q/2)(n_x - n_y)$ is the soliton "eigenvalue." The stability properties of these solutions are then investigated via linear stability analysis.

We begin by separately exploring the one-component TE and TM discrete soliton branches, the $P - \Delta$ diagrams of which are shown in Fig. 1. A close inspection of the eigenvalues (Ω) associated with soliton perturbations reveals that, in its range of existence, the TE family in this AlGaAs array is stable up to a critical power (238 W) at which it *bifurcates into two branches* as can be seen in Fig. 1. Beyond this bifurcation point, the upper branch (dotted line) is the now unstable continuation of the scalar TE soliton family, whereas the lower branch (solid curve) corresponds to a new family of *stable* solutions involving in-phase TE and TM components, i.e., a linearly polarized vector DS. A somewhat similar scenario occurs in the $P - \Delta$ diagram of the TM polarized DSs. In this case, however, the entire TM family (in its range of existence) is always unstable. Note again that after a certain critical power (in this case 257 W) a bifurcation occurs and a new branch corresponding to elliptically polarized vector DSs starts to emerge. This time, however, this elliptically polarized class, where the a_n, b_n components are $\pi/2$ out of phase with respect to each other, is unstable. Even though this picture is reminiscent of similar behavior occurring in birefringent $\chi^{(3)}$ continuous systems [21], there are certain important aspects that are characteristic of discreteness. For example, when propagating in a single waveguide in isolation, both the TE and TM polarizations become unstable [22] for $|a_n|^2, |b_n|^2 \geq 4$ (or 225 W in this case) because of polarization instabilities. Yet, the linearly polarized vector DSs in the array are stable because of interchannel coupling even at high power levels where they are very highly localized.

It is important to note that in the regime where vector DSs are highly confined, their discrete field amplitudes can be well approximated analytically by the following expressions: $X_n = A_0 \exp(-\nu|n|)$ and $Y_n = B_0 \exp(-\mu|n|)$ where $\nu = \cosh^{-1}[(q-1)/2\gamma]$ and $\mu = \cosh^{-1}[(q+1)/2\gamma]$. The soliton amplitudes are obtained from

$$
A_0^2 = \frac{2\gamma[(A \pm B)\sinh(\mu) - \sinh(\nu)]}{(A \pm B)^2 - 1}, \tag{2a}
$$

$$
B_0^2 = \frac{2\gamma[(A \pm B)\sinh(\nu) - \sinh(\mu)]}{(A \pm B)^2 - 1}, \tag{2b}
$$

where the $\pm$ arrangement corresponds, respectively, to the linearly and elliptically polarized vector DS families. The above expressions provide an excellent approximation for the highly confined vector DSs observed in our study.

Figures 2(a) and 2(b), respectively, depict stable propagation of the TE and TM components associated with a linearly polarized highly localized vector DS in an

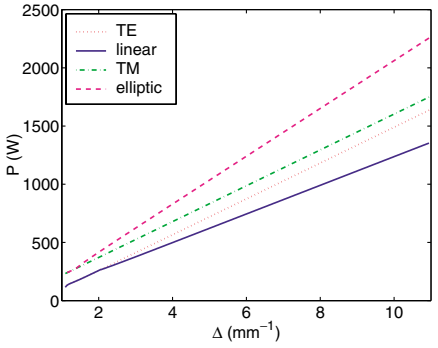

FIG. 1 (color online). $P - \Delta$ diagrams for the linearly polarized (solid line) and elliptically polarized (dashed line) vector discrete solitons as well as for the scalar TE (dotted line) and TM (dot-dashed line) solitons.

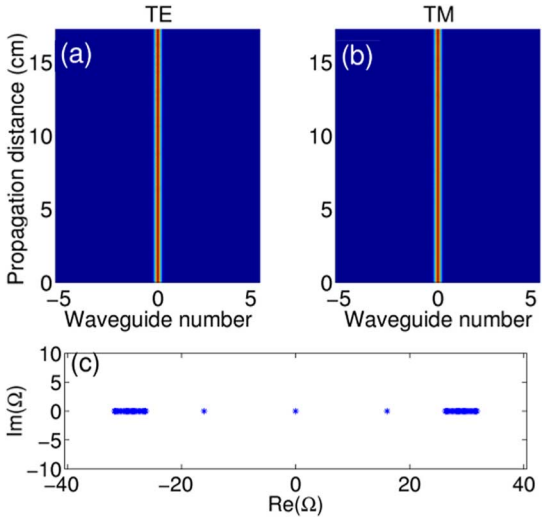

FIG. 2 (color online). Stable propagation of the (a) TE component and (b) TM component of a linearly polarized vector discrete soliton when its total power is 1300 W. The eigenvalues of the perturbed problem are shown in (c).

AlGaAs array. The power conveyed by the TE polarization is, in this case, 766 W and in the TM approximately 540 W. The stability of this vector DS state was also verified by considering the eigenvalues Ω (in the complex plane) of the perturbed problem as shown in Fig. 2(c). As can be seen all eigenvalues are real and thus this composite state is stable, in agreement with the numerical simulations of Figs. 2(a) and 2(b). For this example, the wave-vector shift of this vector DS is $\Delta = 10.6\ \mathrm{mm}^{-1}$. In addition we have studied the stability dynamics of these vector DSs when the in-phase condition between the a_n, b_n components is not exactly met. We found that the vector DS exhibits robustness even when the relative phase difference $\Phi_{\mathrm{TE}} - \Phi_{\mathrm{TM}}$ is of the order of $\pm 20°$,

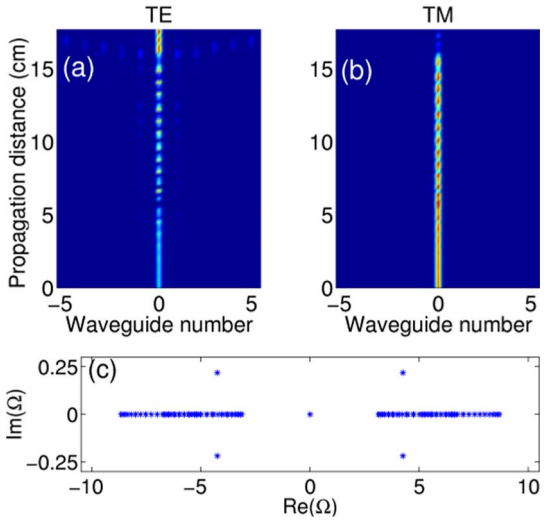

FIG. 3 (color online). Unstable propagation of the (a) TE component and (b) TM component of an elliptically polarized vector discrete soliton when its total power is 430 W. The eigenvalues of the perturbed problem are shown in (c).

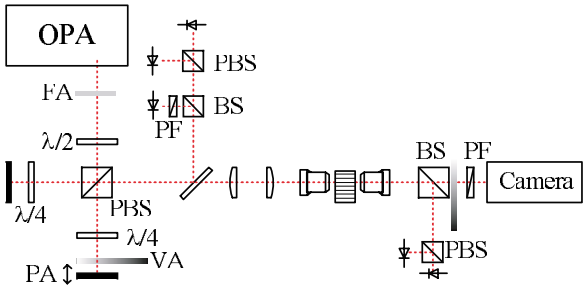

FIG. 4 (color online). The experimental setup is shown (BS: 50/50 beam splitter, PBS: polarizing BS, PF: polarizing filter, FA: fixed attenuator, VA: variable attenuator, PA: piezoelectric actuator, OPA: optical parametric amplifier).

and this is in spite of the fact that some power exchange between the TE and TM components occurs via four-wave mixing effects.

The stability properties and evolution dynamics of an elliptically polarized vector DS were also considered as shown in Fig. 3. In this figure, the TE component carries 92 W and the TM 330 W, and $\Delta \approx 2.2\ \mathrm{mm}^{-1}$. The corresponding eigenvalues of the perturbed problem are shown in Fig. 3(c) where the presence of a complex quartet can be clearly seen. These complex eigenvalues lead to the instabilities seen in Figs. 3(a) and 3(b). In this case, the TM component becomes destabilized and couples most of its power into the TE polarization.

The complete experimental layout is shown in Fig. 4. The light source was a Spectra Physics OPA-800CP which produced 1.1 ps FWHM pulses at a 1 kHz repetition rate. The 1550 nm pulses were attenuated and split into two orthogonal polarizations using a Michelson

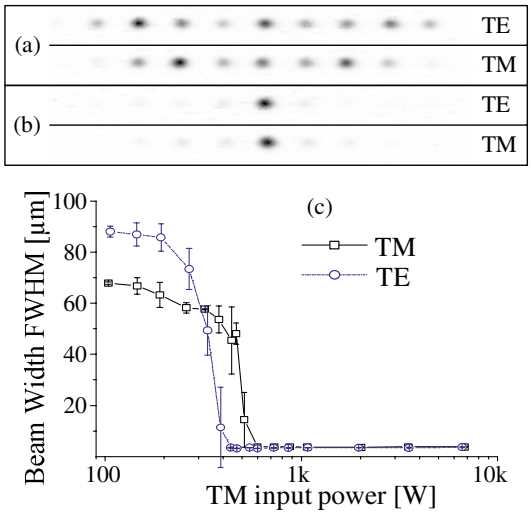

FIG. 5 (color online). Recorded intensity profiles at the output facet of the waveguide array when (a) only a single TE or TM component is present and (b) when both components coalesce to form a vector DS. The power at the input is 650 W for each beam. (c) depicts the FWHM of the output polarization components as a function of TM power for in-phase excitation. The TE power was held fixed at 450 W.

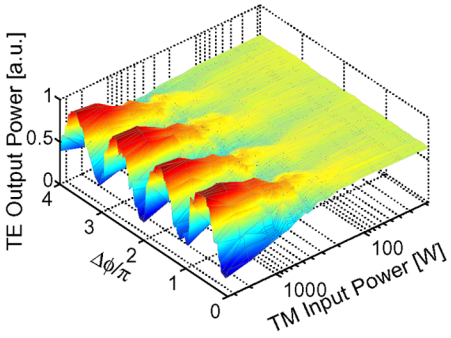

FIG. 6 (color online). Variation of the output TE power as a function of the TM input power and polarization phase difference.

interferometer with a polarizing beam splitter. The optical path length of one arm was adjusted using a piezoelectric actuator. After recombining the beams a small part of the total power was split off to monitor the power in each polarization and the relative phase between them. The main beam was focused on the front surface of the sample in such a way that essentially a single waveguide was excited. The spatial energy distribution at the output surface was observed using an IR-sensitive vidicon camera and the output power in each polarization was measured by germanium detectors.

The recorded intensity profiles at the output facet of the waveguide array when only a single TE or TM component is present are shown in Fig. 5(a). In both cases, the beam (TE or TM) is by itself incapable of forming a DS and as a result it undergoes discrete diffraction (over ten channels) at a peak power of 650 W. On the other hand, when both polarizations are present, mutual trapping occurs, leading to the formation of a highly confined vector DS as can be seen in Fig. 5(b). This takes place when each component carries approximately 650 W. This is in close agreement with the theoretical estimates presented in Fig. 3 where highly confined vector discrete solitons are possible in this AlGaAs array beyond 1200 W total power. Further experiments were performed in order to better understand the mechanism through which strongly localized discrete vector solitons form. These were carried out by combining a TM beam of variable input power with a TE beam kept at a fixed power level in a single channel in the array. Figure 5(c) shows the FWHM of the TE/TM components versus TM input power. When the power of the TM beam exceeded a certain level (500 W), both beams abruptly collapsed into one waveguide channel at the output of the array.

Given that our sample is birefringent, the effect of four-wave mixing on vector discrete solitons was also experimentally investigated. In general this process is periodic and depends on the initial phase difference $\Phi_{TE} - \Phi_{TM}$ between the two polarization components. The dependence of the TE output polarization as a function of the initial relative phase between the two components is demonstrated in Fig. 6. The TE input power was held fixed at 350 W while varying the TM power. The initial phase difference $\Phi_{TE} - \Phi_{TM}$ was varied from 0 to 4π for each TM power level using a piezoelectric actuator. At high powers, both beams collapse into essentially a single channel, leading to a highly localized vector DS. At these power levels, we observe at the output a periodic four-wave mixing gain or loss for the TE component having an oscillation frequency that is twice that associated with the input phase difference. This behavior (i.e., $\exp[2i(\Phi_{TE} - \Phi_{TM})]$) can be anticipated from the four-wave mixing terms in Eqs. (1).

In summary, we have observed for the first time highly localized, vector DSs in AlGaAs nonlinear waveguide arrays.

[1] A. S. Davydov, J. Theor. Biol. **38**, 559 (1973).
[2] D. N. Christodoulides and R. I. Joseph, Opt. Lett. **13**, 794 (1988).
[3] F. Kh. Abdullaev *et al.*, Phys. Rev. A **64**, 043606 (2001).
[4] W. P. Su, J. R. Schieffer, and A. J. Heeger, Phys. Rev. Lett. **42**, 1698 (1979).
[5] S. Somekh *et al.*, Appl. Phys. Lett. **22**, 46 (1973).
[6] N.W. Ashcroft and N. D. Mermin, *Solid State Physics* (Saunders College, Philadelphia, 1976).
[7] F. Lederer, S. Darmanyan, and A. Kobyakov, in *Spatial Optical Solitons*, edited by S. Trillo and W. E. Torruellas (Springer-Verlag, New York, 2001).
[8] H. S. Eisenberg *et al.*, Phys. Rev. Lett. **81**, 3383 (1998); R. Morandotti *et al.*, Phys. Rev. Lett. **86**, 3296 (2001).
[9] T. Pertsch *et al.*, in *Proceedings of Nonlinear Guided Waves and their Applications, Stresa, Italy, 2002* (OSA, Washington, D.C., 2001).
[10] J.W. Fleischer *et al.*, Nature (London) **422**, 147 (2003); N. K. Efremidis *et al.*, Phys. Rev. E **66**, 046602 (2002).
[11] Y. S. Kivshar, Opt. Lett. **18**, 1147 (1993).
[12] D. Mandelik *et al.*, Phys. Rev. Lett. **90**, 053902 (2003).
[13] S. Darmanyan *et al.*, Phys. Rev. E **57**, 3520 (1998); A. Kobyakov *et al.*, Opt. Quantum Electron. **30**, 795 (1998).
[14] D. N. Christodoulides and R. I. Joseph, Opt. Lett. **13**, 53 (1988); M. Haelterman *et al.*, Opt. Lett. **18**, 1406 (1993); Y. Silberberg and Y. Barad, Opt. Lett. **20**, 246 (1995).
[15] G. I. Stegeman and M. Segev, Science **286**, 1518 (1999).
[16] J. U. Kang *et al.*, Phys. Rev. Lett. **76**, 3699 (1996); N. Shalaby and A. J. Barthelemy, IEEE J. Quantum Electron. **28**, 2736 (1992).
[17] M. Mitchell *et al.*, Phys. Rev. Lett. **80**, 4657 (1998); Z. Chen *et al.*, Opt. Lett. **21**, 1436 (1996).
[18] T. Peschel, U. Peschel, and F. Lederer, Phys. Rev. E **57**, 1127 (1998).
[19] M. J. Ablowitz and Z. H. Musslimani, Phys. Rev. E **65**, 056618 (2002).
[20] D. N. Christodoulides and E. D. Eugenieva, Phys. Rev. Lett. **87**, 233901 (2001).
[21] E. A. Ostrovskaya *et al.*, J. Opt. Soc. Am. B **14**, 880 (1997); R. R. Malendevich *et al.*, J. Opt. Soc. Am. B **19**, 695 (2002).
[22] H. G. Winful, Opt. Lett. **11**, 33 (1986); S. Trillo *et al.*, Appl. Phys. Lett. **49**, 1224 (1986).